ALEPH/97-065
PHYSIC 97-057
June 18, 1997

Progress report for WWγ gauge coupling study in Single Photon production at 161 and 172 GeV

J. Boucrot, A. Jacholkowska, Z.Wąs[1]
Laboratoire de l'Accélérateur Linéaire
91405 Orsay Cedex, France

Abstract

A study of single and multiphoton events has been done for the data sample obtained with ALEPH at 161 and 172 GeV in 1996. The anomalous coupling parameters are constrained, leading to the values

$$\Delta\kappa_\gamma = -0.5^{-2.8}_{+3.3}(\mathrm{stat}) \pm 0.75(\mathrm{syst})$$
$$\lambda_\gamma = 0. \pm 5.8(\mathrm{stat}) \pm 0.75(\mathrm{syst})$$

The Monte Carlo study of error calibrations confirms the reliability of the procedure used to obtain these results.

[1]Permanent address: Inst. of Nuclear Physics, Cracow, Poland

1 Introduction

The study of the reaction $e^+e^- \to \nu\overline{\nu}\gamma(\gamma)$ at LEP 2 energies [1], [2] is a possible domain of investigation for the non-abelian sector of the Standard Model. The advantadges of this channel are as follows:

- in the Lagrangian, only 2 parameters, namely $\Delta\kappa_\gamma$ and λ_γ describe the anomalous couplings;
- there is no model dependence;
- this study is complementary to the results of the Tevatron experiments dealing with energetic W's;
- it is specially interesting when combined with the α_ϕ model in the W pair channel or in the single W channel;
- it is possible to use a weighting procedure for Monte-Carlo studies, due to the bilinear form of the matrix elements as a function of the anomalous coupling parameters.

The disadvantages come from the low cross sections, and from the irreducible background given by the reaction:

$$e^+e^- \to Z^0 + n\gamma, n \geq 2$$

Below, a detailed study of the sensitivity to anomalous couplings is presented, as well as an optimisation of the cuts used in the analysis.

2 Weighting method in KORALZ

To obtain a description of the anomalous couplings in the simulation, a procedure has been used where each event is assigned a weight which is a function of $\Delta\kappa_\gamma$ and λ_γ.

This method of correlated samples provides the lowest error, as the statistical error affects only the differences between Standard Model and “anomalous” distributions.

The matrix element is linear in $\Delta\kappa_\gamma$ and λ_γ:

$$A = A_{SM} + \Delta\kappa_\gamma A_1 + \lambda_\gamma A_2$$

Thus the cross-section differential distributions are bilinear forms of $\Delta\kappa_\gamma$ and λ_γ. It follows that it is sufficient to store weights for only six configurations in the $(\Delta\kappa_\gamma, \lambda_\gamma)$ plane, as this allows to recalculate matrix elements squared $\mathrm{S_i}(\Delta\kappa_\gamma, \lambda_\gamma)$ for any other value of $\Delta\kappa_\gamma and \lambda_\gamma$ using the formula:

$$S_i = (C_{ij})^{-1} \times D_j$$

where D_j is its value for a given $(\Delta\kappa_\gamma\ ,\ \lambda_\gamma)$, and

$$C^{-1} = \begin{pmatrix} 1 & 0 & 0 & 0 & 0 & 0 \\ -\frac{1}{\Delta\kappa_\gamma{}^2} & \frac{1}{2\Delta\kappa_\gamma{}^2} & \frac{1}{2\Delta\kappa_\gamma{}^2} & 0 & 0 & 0 \\ -\frac{1}{\lambda_\gamma{}^2} & 0 & 0 & \frac{1}{2\lambda_\gamma{}^2} & \frac{1}{2\lambda_\gamma{}^2} & 0 \\ 0 & -\frac{1}{2\Delta\kappa_\gamma} & \frac{1}{2\Delta\kappa_\gamma} & 0 & 0 & 0 \\ 0 & 0 & 0 & -\frac{1}{2\lambda_\gamma} & \frac{1}{2\lambda_\gamma} & 0 \\ \frac{1}{\lambda_\gamma\Delta\kappa_\gamma} & 0 & -\frac{1}{\lambda_\gamma\Delta\kappa_\gamma} & 0 & -\frac{1}{\lambda_\gamma\Delta\kappa_\gamma} & \frac{1}{\lambda_\gamma\Delta\kappa_\gamma} \end{pmatrix}$$

In the present version of KORALZ, the following $(\Delta\kappa_\gamma, \lambda_\gamma)$ pairs of values were used:

$\Delta\kappa_\gamma$:	0.	-10.	10.	0.	0.	-10.
λ_γ:	0.	0.	0.	-10.	10.	10.

The weighting procedure allows to use only one simulation; note that the formula given above extends in a natural way to any cross section and differential distribution, within arbitrary but fixed cuts.

In the $e^+e^- \rightarrow \nu\overline{\nu}\gamma(\gamma)$ reaction, the contributing graphs correspond to the Z^0 production in the s-channel and to the W exchange in the t-channel. As the Z^0 mass and width are known very precisely, the results depend very weakly on the input parameters.

3 Sensitivity of the cross-sections to the anomalous couplings

In this study, two kinematical variables of the photon have been used: the scaled energy x_E and the scale transverse momentum x_t. As these are not invariants, the domains of these variables vary with energy.

Fig. 1 shows the variation of calculated weights from anomalous coupling amplitudes, as a function of x_E for each event. It is clearly seen that the sensitivity to anomalous couplings decreases in the region of the Z^0 peak ($0.6 < x_E < 0.75$).

Two regions of interest have been studied for the optimisation of the sensitivity to the anomalous coupling parameters and statistical meaning of the samples:

region (1) where

$$x_E < 0.585 \text{ (161 GeV)}$$
$$x_E < 0.625 \text{ (172 GeV)}$$

corresponding to the photon energy:

$$E_\gamma < E_\gamma(Z^0) + 3\Gamma_Z$$

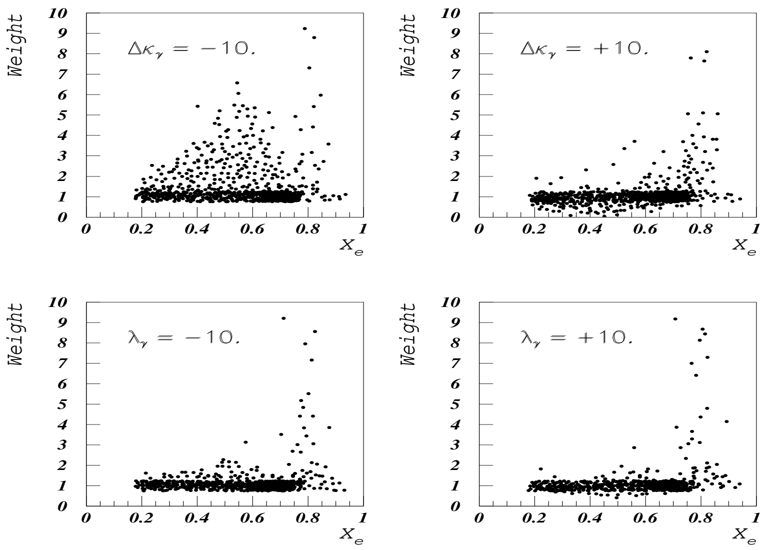

Figure 1: Calculated weights for several anomalous couplings $\Delta\kappa_\gamma$ and λ_γ, as a function of the scaled energy x_E

and region (2) where

$$x_E > 0.685 \ (161 \text{ GeV})$$
$$x_E > 0.725 \ (172 \text{ GeV})$$

corresponding to:

$$E_\gamma > E_\gamma(Z^0) + 0.5GeV$$

Fig. 2 presents the predicted sensitivity for both samples. The estimators used were :

$$S^{\pm}_{\Delta\kappa_\gamma} = \frac{\sigma(\Delta\kappa_\gamma = \pm 10., \lambda_\gamma = 0.)}{\sigma_{SM}} - 1.$$

$$S^{\pm}_{\lambda_\gamma} = \frac{\sigma(\Delta\kappa_\gamma = 0., \lambda_\gamma = \pm 10.)}{\sigma_{SM}} - 1.$$

The dependence for positive or negative values of $\Delta\kappa_\gamma$ has to be studied separately due to the strong asymmetry of $\sigma(\Delta\kappa_\gamma)$. As a consequence, it is necessary to make a separate analysis of the two regions, leading to a combination of results at the last step of the likelihood fit.

For all estimators, a substantial increase of the sensitivity is observed, showing that in this study the c.m.s. energy is of the same importance as the collected luminosity.

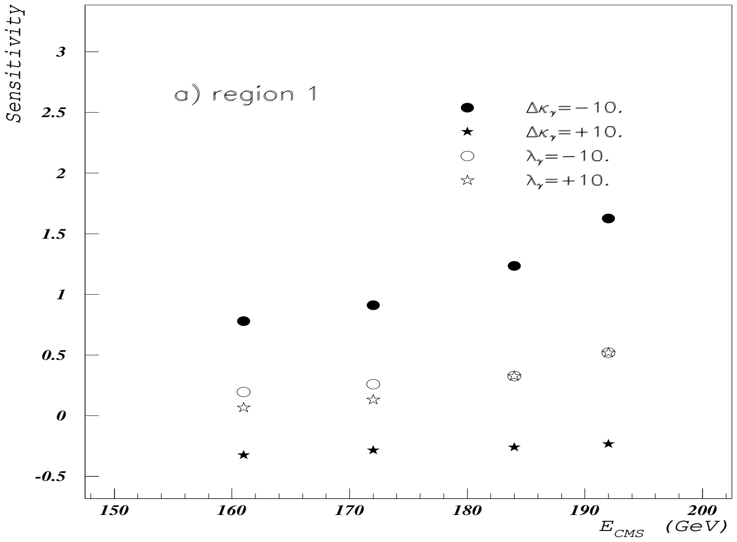

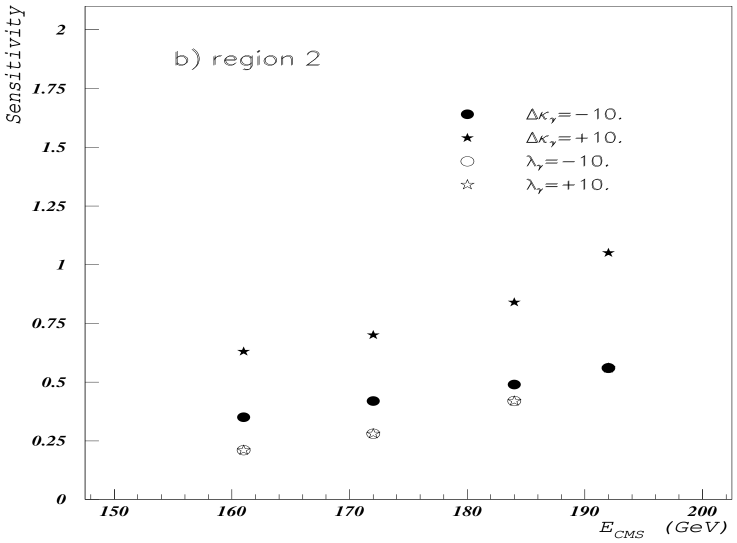

Figure 2: Sensitivity $S^{\pm}_{\Delta\kappa_\gamma}$ and $S^{\pm}_{\lambda_\gamma}$ as defined in the text, as a function of the center of mass energy, for Regions 1 and 2

4 Data analysis

4.1 Selections and cuts

The data sample is the same as described in [3] at 161 and 172 GeV.

Here, only changes in the photon energy measurement, and additional cuts with respect to the previous note [3] are described.

- Photon energy measurement:

  An "official" procedure for the measurement of the single photon energy has been used, based on the estimation from the PECO clusters outside cracks, and adding to the PECO energy the hadronic cluster energy in the crack regions. Thus a better resolution is obtained for high energy photons, as tested on QED photon samples [4].

- The angular cut has been raised to 20°, to avoid possible contributions from radiative Bhabhas or 3-photon QED events.

- In the selection of 2-photon events, the angular cut of 20° has been required for both photons.

The final acceptance cuts are therefore:

$$E_\gamma > 0.1\sqrt{s},$$
$$\theta_\gamma > 20^\circ$$
$$x_T = p_T^\gamma / E_{beam} > 0.15.$$

Table 1 shows the data and Monte Carlo event samples used in this analysis.

Table 1: Data and Monte Carlo samples

Energy (GeV)	Luminosity (pb^{-1})	Data N Events	Monte Carlo N Events
161	11.0	37	$4\ 10^4$
172	10.7	31	$8\ 10^4$
Total	21.7	68	$12\ 10^4$

Fig. 3 shows the distribution of the scaled energy for data, compared to Standard Model predictions. A good compatibility is observed. As stated in Sec 3, only events with $x_E < 0.6$ and $x_E > 0.7$ will be used in the following analysis.

4.2 Scaled energy

The possible contributions to the $e^+e^- \to \gamma(\gamma) + X$ channel, other than $X \to \nu\overline{\nu}$, may come from radiative Bhabhas, QED multiphotons or SUSY particles. The angular and energy cuts can eliminate the first two contributions. The SUSY particles

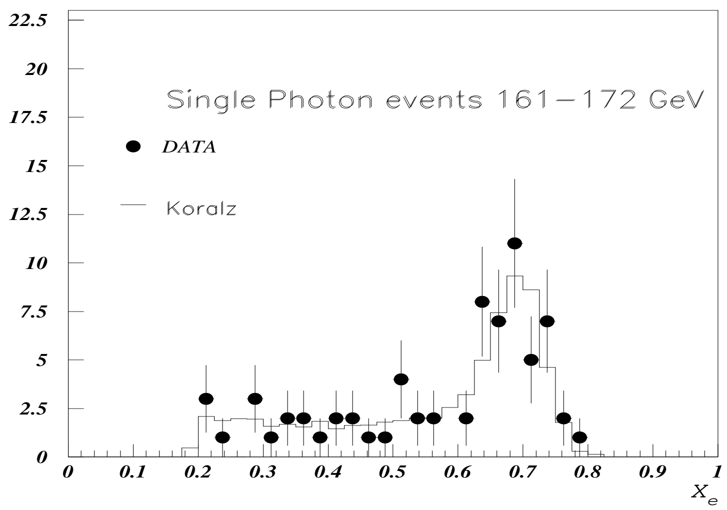

Figure 3: Distribution of the scaled energy x_E, for data and Monte Carlo

have not yet been observed, however they may interfere in the anomalous coupling interpretation of the deviations from the Standard Model.

The irreducible background in region 1 comes from the multiphoton Z^0 return. It also introduces a correction factor on the observed number of events in region 2.

The KORALZ simulation of Higher Order effects gives about $+100\%$ correction for the cross-section in region 1, and about -30% correction in region 2.

A theoretical estimate of the error on these correction factors is of the order of $10-15\%$. However, only comparisons with complete calculations from the exact matrix elements (not present in KORALZ) for the 2 and 3 hard bremsstrahlung photons will allow a satisfactory estimation of this uncertainty. For the c.m.s. energy of LEP 1, such tests were performed and published for 2 hard photons configurations. It is straightforward to extend these tests to LEP 2 energies. The case of 3 hard photons is somewhat more complicated. A discussion of the uncertainty due to the implementation of the matrix elements with anomalous couplings for the multiphoton events will be also presented elsewhere.

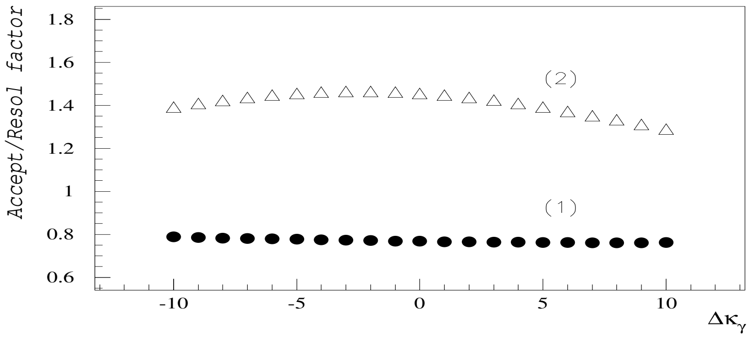

Figure 4: Acceptance and resolution factors, as a function of $\Delta\kappa_\gamma$

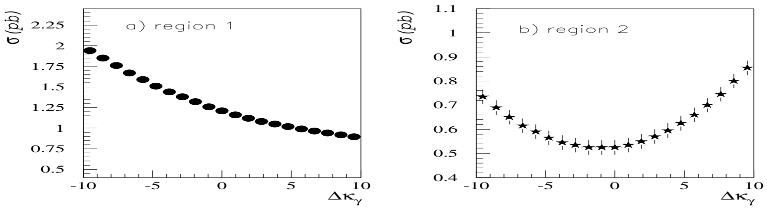

Figure 5: Cross-sections as a function of $\Delta\kappa_\gamma$, for the two kinematical regions

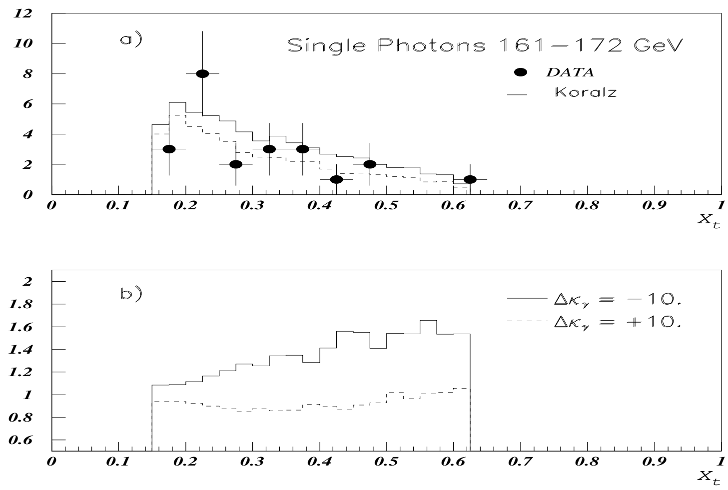

Figure 6: Region 1 a): x_e distributions from data and from the Standard Model prediction, b): ratio of the predictions for $\Delta\kappa_\gamma = \pm 10$ with respect to the S.M.

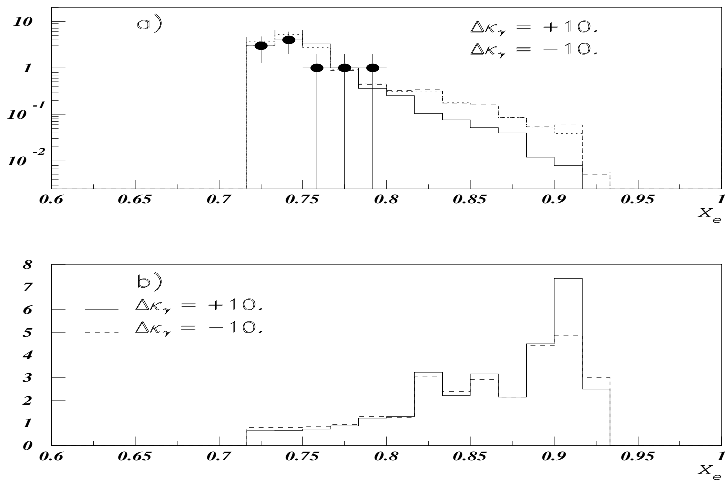

Figure 7: Region 2 a): x_T distributions from data and from the Standard Model prediction, b): ratio of the predictions for $\Delta\kappa_\gamma = \pm 10$ with respect to the S.M.

5 Likelihood fit

The limits for anomalous coupling parameters have been derived from the generalised likelihood expression:

$$L = \frac{(\mathrm{N_{th}})^{\mathrm{N_{obs}}}\, \mathrm{e}^{-\mathrm{N_{th}}}}{\mathrm{N_{obs}}!} \prod_{i=1}^{Nobs} \mathrm{P_i}$$

$\mathrm{P_i}$ is the probablitiy obtained from distributions for each event.

This likelihood formula contains two parts: the first one concerning the number of observed events, the second one being related to differential distributions for each kinematic region. This leads to an expression containing 4 terms:

$$\log(\mathrm{L}) = \log\left(\frac{(\mathrm{N_{th}})^{\mathrm{N^{(1)}_{obs}}}\, \mathrm{e}^{-\mathrm{N_{th}}}}{\mathrm{N^{(1)}_{obs}}!}\right) + \log\left(\frac{(\mathrm{N_{th}})^{\mathrm{N^{(2)}_{obs}}}\, \mathrm{e}^{-\mathrm{N_{th}}}}{\mathrm{N^{(2)}_{obs}}!}\right) + \sum \log(\mathrm{P_i^1}) + \sum \log(\mathrm{P_i^2})$$

where $\mathrm{N_{th}}$ is the expected number of events in each region:

$$\mathrm{N_{th}} = \text{Luminosity} \times \text{Accept}(\Delta\kappa_\gamma) \times \sigma(\Delta\kappa_\gamma) + \text{Background}$$

Fig 4 shows the acceptance as a function of $\Delta\kappa_\gamma$ for low and high energy photons.

The treatment of the two kinematic regions differs in the following points:

- Region 1 (low energy photons) : the contribution from Higher Order radiative corrections is put in the fit as a constant term determined by the Monte Carlo; this procedure gives a much lower uncertainty on these corrections. The scaled p_t variable, x_t, is used as a kinematical variable in the fit. Fig 6a and 6b present the experimental x_t distribution, compared to the predictions for $\Delta\kappa_\gamma = \pm 10$, and their ratio with respect to the Standard Model prediction.
- Region 2 (high energy photons) : the Higher Order radiative corrections effect is to decrease the number of expected events by 30 %. The kinematic variable used for the probability determination is the scaled energy x_E. Fig. 7a presents the measured x_E distribution compared to those predicted for $\Delta\kappa_\gamma = \pm 10$ values, and Fig 7b their ratio with respect to the Standard Model prediction.

The form of both cross-sections (displayed in Fig. 5) and distribution shapes differ in the two regions. As it is monotonous and linear for $\Delta\kappa_\gamma > 0.$ and $\Delta\kappa_\gamma < 0.$ for the low energy region, only one solution is expected for the $\Delta\kappa_\gamma$ fit. In case of high energy photons, the dependences are quadratic and two or one solutions are expected, the case of one solution corresponds to $\Delta\kappa_\gamma = 0$.

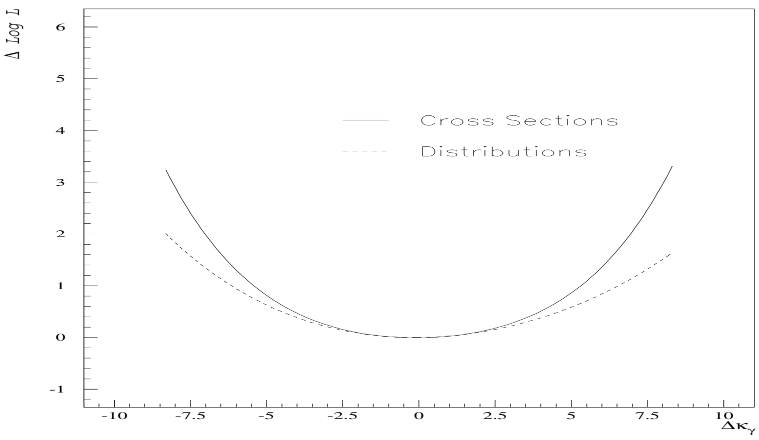

Figure 8: Likelihood curves for the fit of $\Delta\kappa_\gamma$ at $\lambda_\gamma = 0$.

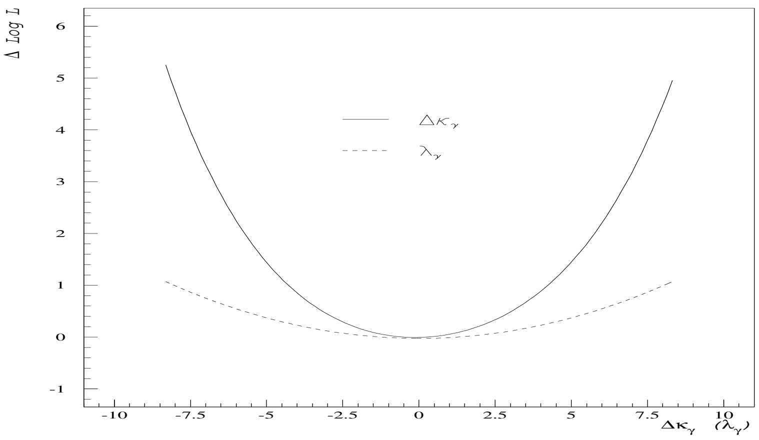

Figure 9: Likelihood curves for the fit of λ_γ and $\Delta\kappa_\gamma$.

6 Results

Fig. 8 presents the -Δlog(L) curves corresponding to the fit of $\Delta\kappa_\gamma$ at $\lambda_\gamma = 0.$, the cross-section and distribution terms being separated. The 4th degree polynomial is needed to represent these -Δlog(L) functions. At present, the cross-section term gives the dominant contribution.

Fig. 9 presents the -Δlog(L) functions for $\Delta\kappa_\gamma$ fitted at $\lambda_\gamma = 0.$, and for λ_γ fitted at $\Delta\kappa_\gamma = 0.$.

The constraints from these fits for anomalous couplings are:

$$\Delta\kappa_\gamma = -0.5^{-2.8}_{+3.3}(\text{stat}),\ \text{if}\ \lambda_\gamma = 0.$$
$$\lambda_\gamma = 0. \pm 5.8\text{stat},\ \text{if}\ \Delta\kappa_\gamma = 0.$$

7 Systematic errors

7.1 Error calibration

A total number of 42 simulated Monte Carlo samples have been used to estimate possible systematic deviations for the anomalous parameter determination. This also allows to cross-check the validity of the errors given by the likelihood fit.

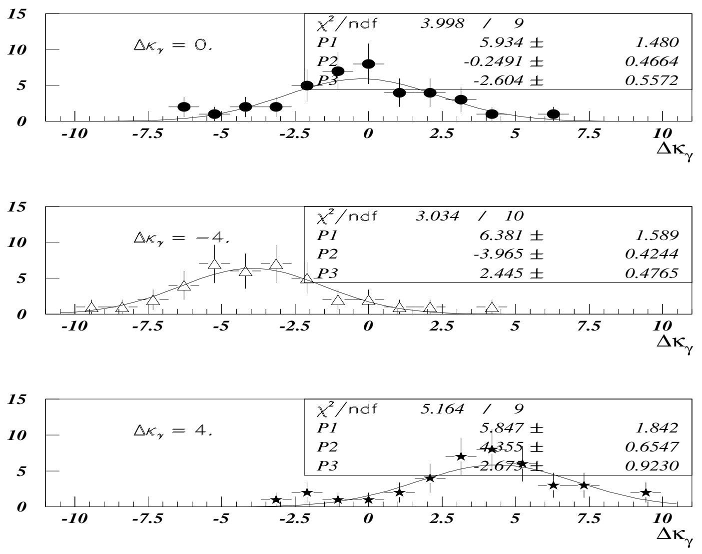

Figure 10: Values of $\Delta\kappa_\gamma$ reconstructed for input values of 0, -4 and 4

The size of the Monte Carlo samples has been optimized to minimize the inhomogeneity of the weights in the sample : 4 times the data for Region 1 and 12 times for Region 2. It can be noticed that large weight values for high energy photons correspond to $\theta_\gamma > 40°$.

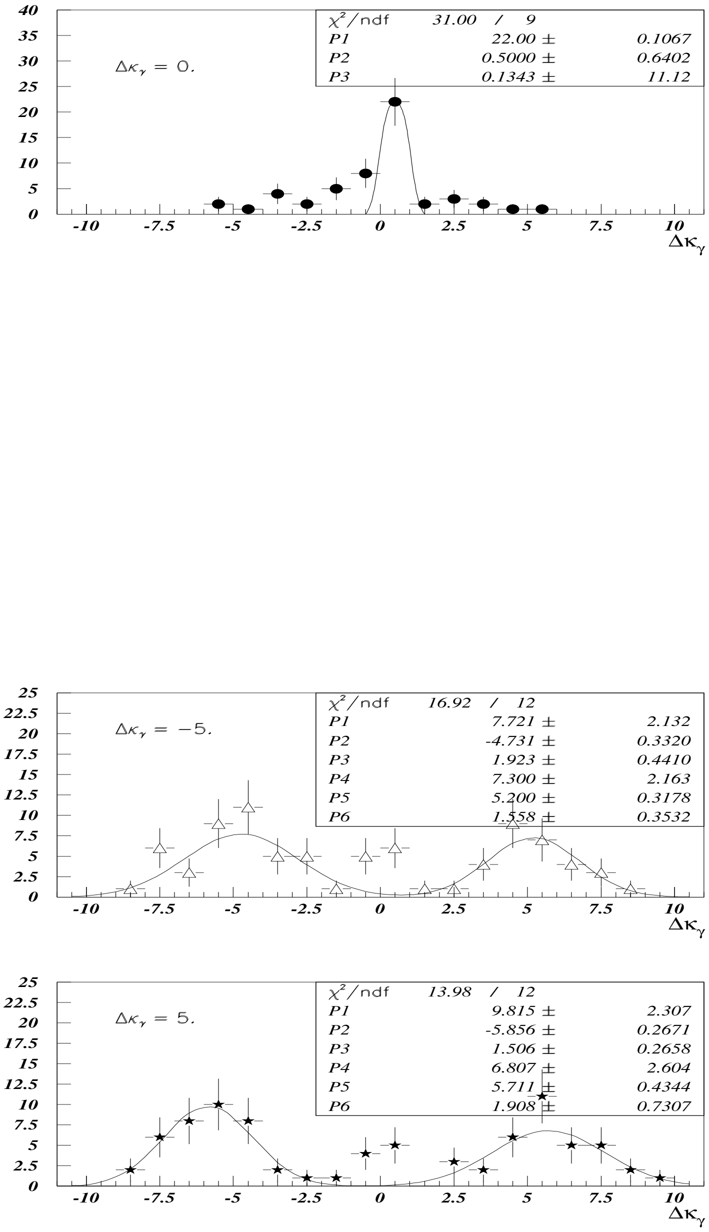

Figure 11: Reconstructed values of $\Delta\kappa_\gamma$ for input values of 0, -5 and 5

The calibration has been performed for the distribution part of the fit.

Fig. 10 presents the values of $\Delta\kappa_\gamma$ reconstructed for initial values $\Delta\kappa_\gamma = -4$, 0 and 4. No systematic deviation is observed and the widths measured with the Monte Carlo samples confirm the error estimation done on the data.

Fig 11 shows the values of $\Delta\kappa_\gamma$ reconstructed for initial values $\Delta\kappa_\gamma = -5$, 0 and 5. A two standard deviation deviation from linearity is observed for $\Delta\kappa_\gamma > 0$. The errors seem to be correctly estimated in the data fit. The number of solutions with a reconstructed $\Delta\kappa_\gamma = 0$ for initial values $\Delta\kappa_\gamma = -5$ or $+5$ is $20 \pm 5\%$, as expected, confirming that the error determination is correct.

7.2 Systematic errors

The main contributions to the systematic uncertainty on the determination of $\Delta\kappa_\gamma$ and λ_γ are summarised in Table 1.

Table 2: Contributions to the systematic uncertainty

Uncertainty	Error
Energy calibration $\pm 2\%$	± 0.5
Background < 1 event	< 0.5
H.O. corrections	± 0.2
Fit procedure	- 0.2
Total	0.75

The main contribution to the systematic error comes from the energy calibration for the extra high energy photons. Here, the redundancy of the pad/wire information plays a crucial role. In the future, all the other contributions will substantially decrease while increasing the integrated luminosity. The energy calibration will be checked with a large QED photon sample.

8 Conclusions

The anomalous coupling parameters $\Delta\kappa_\gamma$ and λ_γ have been constrained from single photon production at 161 and 172 GeV. The results from the fit to the cross-sections and to the p_t and energy distributions of the photons (for $\Delta\kappa_\gamma$) are:

$$\Delta\kappa_\gamma = -0.5^{-2.8}_{+3.3}(\mathrm{stat}) \pm 0.75(\mathrm{syst}),\ \text{if } \lambda_\gamma = 0.$$
$$\lambda_\gamma = 0. \pm 5.8(\mathrm{stat}) \pm 0.75(\mathrm{syst}),\ \text{if } \Delta\kappa_\gamma = 0.$$

The Monte Carlo error calibration confirms the fitted error values from the fit on the data sample for the shape variation of the distributions. The results are linear ($\pm 2\sigma$) in the fitted parameters.

The future developments will concentrate on a full two-parameter fit to the double differential cross-section $d^2\sigma/d\theta_\gamma dE_\gamma$. The systematic uncertainties should go down with increasing statistics, the dominating one being the energy calibration for the energetic photons.

The prospects of this measurement lie in combinating it with the results from the W pair channel and the single W channel.

9 Acknowledgements

We would like to thank J. Kalinowski for suggesting the study of this subject and for providing us with the anomalous coupling matrix elements.

References

[1] J. Abragam, J.Kalinowski, P.Sciepko, Phys. Lett. **B 339** (1994) 136.
F. Berends *et al.*, Nucl. Phys. **B 301** (1988) 583.

[2] Physics at LEP2, CERN 96-01, 525.
D. Choudhbury, J.Kalinowski MPI-PTH /96-73, IFT-96/17.

[3] J.Boucrot, A.Jacholkowska, P.Heusse note ALEPH/97-015 (PHYSIC 97-012), February 1997.

[4] J. Dann, private communication.